RESEARCH ARTICLE

Optimal Control Simulation Predicts Effects of Midsole Materials on Energy Cost of Running

Eva Dorschky[a], Daniel Krüger[b], Nicolai Kurfess[a], Heiko Schlarb[c], Sandro Wartzack[b], Björn M. Eskofier[a], Antonie J. van den Bogert[d]

[a]Machine Learning and Data Analytics Lab, [b]Engineering Design, Friedrich-Alexander-Universität Erlangen-Nürnberg (FAU), Germany;
[c]FUTURE TEAM, adidas AG, Germany;
[d]Mechanical Engineering Department, Cleveland State University, USA

ABSTRACT

Testing sports equipment with athletes is costly, time-consuming, hazardous and sometimes impracticable. We propose a method for virtual testing of running shoes and predict how midsoles made of BOOST$^{\mathrm{TM}}$ affect energy cost of running. We contribute a visco-elastic contact model and identified model parameters based on load-displacement measurements. We propose a virtual study using optimal control simulation of musculoskeletal models. The predicted reduction in energy cost of $\sim 1\%$ for BOOST in comparison to conventional materials is consistent with experimental studies. This indicates that the proposed method is capable of replacing experimental studies in the future.

KEYWORDS

Virtual Design, Footwear, Running, Musculoskeletal Simulation

---

Contact: eva.dorschky@fau.de

This is an original manuscript of an article published by Taylor & Francis in Computer Methods in Biomechanics and Biomedical Engineering on 16 April 2019, available online: https://doi.org/10.1080/10255842.2019.1601179.

1. Introduction

Sports products are typically developed in an iterative process by prototyping and testing. This process suffers from high costs and long lead times, conflicting with short development cycles. Computer simulations that can predict the effect of design parameters on human movement and performance will revolutionize the development process. Different shoe concepts can be studied and validated in the virtual stage, with the consequence that a more mature concept with higher quality can enter the market.

The sports industry uses virtual prototypes (finite element models) to simulate the mechanical characteristics of sports products. A few attempts have been made to integrate a biomechanical analysis in the finite element framework by investigating dynamic finite element models (Cheung and Zhang 2006; Hannah et al. 2016; Kim et al. 2012). However, these methods only consider movements of single parts of the body (like foot or lower leg movements) and can not yet predict full-body human responses, i.e., kinematic, kinetic, and metabolic changes due to design parameters. Apart from that, musculoskeletal simulation is employed to study full-/lower-body kinematics and kinetics of running. For example, Wright et al. (Wright et al. 1998) and Miller et al. (Miller and Hamill 2009) modeled footwear as nonlinear visco-elastic elements and examined the human response to changing shoe stiffness. Both studies were based on measurement data of optical motion capture systems, which was tracked to derive muscle stimulation patterns of running (Miller and Hamill 2009). Using these derived muscle controls and given initial kinematic conditions, forward dynamic simulations were performed with different contact models for varying shoe stiffness. The predefined muscle controls are inaccurate as muscle activity can change due to changes in footwear (Wakeling et al. 2002).

We want to predict motion trajectories and muscle controls simultaneously without the need of predefined kinematic states or muscle controls. Former work has shown that human motion can be simulated by solving an optimal control problem: Find a motion trajectory and muscle controls that minimize a physically motivated cost function such as minimal muscular effort, cost of transport or mechanical loading (van den Bogert et al. 2011; Wang et al. 2012; Lin et al. 2018). Tracking data of human motion was included in the cost function to ensure that the simulated motion was realistic. van den Bogert et al. (2011) proposed an efficient method for solving such optimization problems using direct collocation to make it feasible for design applications. They were able to predict changes of human kinematics and energy cost due to varying mass properties of wearable equipment (van den Bogert et al. 2012). The effects of running shoes and elastic and dissipative material properties were not considered. They evaluated energy cost based on positive mechanical work. In addition, we want to predict metabolic changes to estimate the economy of running with different footwear. If athletes can run with lower energetic cost at a specified velocity, then they should be able to run faster with their existing physiological capacities (Hoogkamer et al. 2016). Thus, running economy gives an indication on running performance which is a key objective in sports product design and should be considered as an evaluation parameter. Miller and Hamill (2015) examined footfall patterns of shod and barefoot running based on different optimality principles. They only compared shod and barefoot running and did not consider differences in footwear. Moreover, they focused on kinematic changes (rearfoot vs. non-rearfoot running) and did not evaluate performance measures. We further investigated direct collocation simulation to study footwear effects on running performance.

A major drawback of most simulation studies is that only one generic model was used (van den Bogert et al. 2012; Dorn et al. 2015). We want to simulate multiple musculoskeletal models to ensure that the simulation results are insensitive to model parameters and to represent a population of runners. Esposito and Miller (2018) conducted a simulation study with 25 virtual subjects to predict metabolic cost of walking pre- and post-limb loss. They randomized muscle parameters to represent a population of young adult males. In the optimal control simulation, they tracked the between-subjects mean of experimental gait data. Averaging data across multiple subjects could lead to unnatural movement patterns and does not reflect the variability of human movement. Especially in our case, we want to simulate different running styles like rear-foot, mid-foot and fore-foot running. The individual running pattern is hardly affected by small changes in footwear according to the preferred movement path paradigm (Nigg et al. 2017). Therefore, we propose a new virtual study design that uses randomized virtual subjects to represent a population of runners while considering different movement patterns. We avoid any data acquisition by using a public available data set for tracking various running biomechanics (Fukuchi et al. 2017).

Current literature does not provide methods to predict the effect of footwear on human performance by computer simulation. Our objective is to present a methodology for this and evaluate it for a use case. In particular, we predict the influence of midsole materials on energy cost of running using optimal control simulation (van den Bogert et al. 2011; van den Bogert et al. 2012). The contribution of this work involves (i) a novel ground-contact model to capture shoe characteristics (see Sec. 2.1) and (ii) a virtual study design to replace experimental studies (see Sec. 2.2).

2. Methods

Fig. 1 shows an overview of the proposed methods. We compared the influence of two midsole materials on running economy: a midsole out of BOOST^{TM} (SOFT) versus a common midsole material, ethyl vinyl acetate (CONTROL). We compared two running shoes that only differed in their midsole material. The same study was performed experimentally by Worobets et al. (2014). They showed that the more compliant and resilient shoe midsoles (BOOST^{TM} (SOFT)) reduce the energetic cost of running by approx. 1%. We conducted an equivalent simulation study and compared the results to the experimental results.

2.1. Ground-Contact Model

This section describes the ground-contact model and how we captured the characteristics of the two midsole materials. We performed multiple mechanical force-deformation measurements to identify the forefoot (FF) and rearfoot (RF) area of the shoes (see Sec. 2.1.1). The respective visco-elastic behavior (stiffness and damping) was described by fitting a polynomial regression model to the force-deformation measurements (see Sec. 2.1.2).

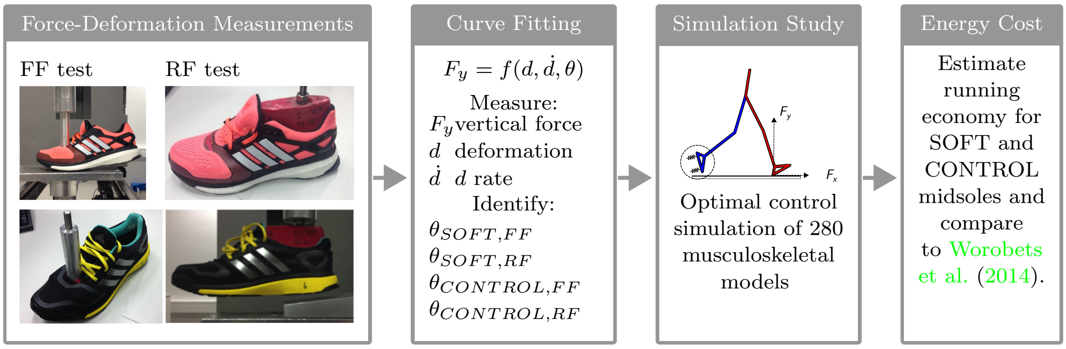

Figure 1.: Overview of methods: Two identical running shoes with different midsole materials, SOFT and ethyl vinyl acetate (CONTROL), were characterized by force-deformation measurements with different test setups for the forefoot (FF) and rearfoot (RF) (see Sec. 2.1.1). Based on the measurement data, we created a contact-response model and identified the model parameters for forefoot (FF) and rearfoot (RF) of SOFT and CONTROL (see Sec. 2.1.2). Then, we ran a simulation study with 280 randomized musculoskeletal models and estimated the change in energy cost for running with SOFT midsoles (see Sec. 2.2).

2.1.1. Force-Deformation Measurements

We performed different tests for the FF and RF to consider the different material thickness and weight distribution during a gait cycle. Therefore, we mounted the running shoes in a servo-hydraulic testing machine (Instron®). The machine can generate high-dynamic load patterns that are applied to the shoe via a stamp or a last. It further determines the resulting deformation of the sole material. We programmed the machine to simulate typical load and unload patterns of human heel-to-toe running, where different loads were applied to the FF and RF according to Tab. 1.

Fig. 2a shows the standard setup parameters for RF-1 and FF-1: The maximum load, F_{max}, is reached at loading time, t_{load}, and returns to zero at unloading time, t_{unload}. We used a haversine function for smoothing resulting in an applied force as shown in Fig. 2b. We chose the standard setup parameters to imitate a typical loading pattern of a 75 kg heel-striker with an average ground contact time (Nigg 2010), as indicated as dotted line in Fig. 2b. Afterwards, we altered these parameters to imitate running of more lightweight and heavier persons and different running styles resulting in variations of the ground reaction force (GRF) profile. The maximum loading, F_{max}, was varied to a large extent in between 50% and 200% of the default parameter to allow for a more general contact model (see Tab. 1). Moreover, we varied t_{load} and t_{unload} by 75%, 100%, 125% to simulate different running speeds. Additionally, we performed

Table 1.: Setup parameters of force-deformation tests for the rearfoot (RF) and forefoot (FF) according to Fig. 2a.

Measurement ID	Repetitions	F_{max} (N)	t_{load} (ms)	t_{unload} (ms)
RF-1	20	1800	35	95
RF-2	20	900	35	95
RF-3	20	1350	35	95
RF-4	20	1800	35	95
RF-5	20	2250	35	95
RF-6	20	2700	35	95
RF-7	20	3600	35	95
RF-8	20	1800	26	71
RF-9	20	1800	44	119
RF-10	20	1800	100	200
FF-1	20	2000	100	200
FF-2	20	1000	100	200
FF-3	20	1500	100	200
FF-4	20	2000	100	200
FF-5	20	2500	100	200
FF-6	20	3000	100	200
FF-7	20	4000	100	200
FF-8	20	2000	35	95
FF-9	20	2000	75	150
FF-10	20	2000	125	250

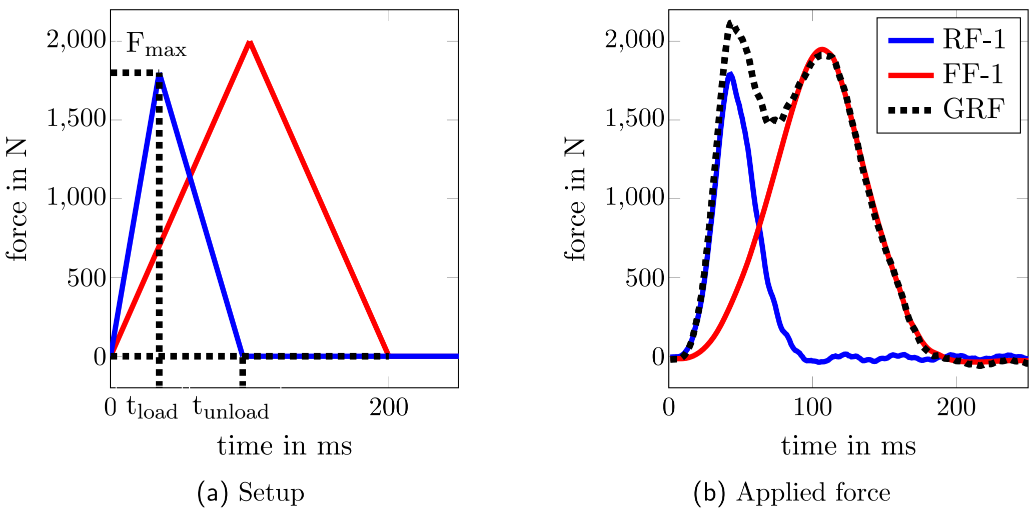

Figure 2.: Example setup (a) for force-deformation tests for the rearfoot (RF) (blue) and forefoot (FF) (red), RF-1, FF-1 in Tab. 1. The summation of the applied forces (b) leads to typical ground reaction force (GRF) patterns of running.

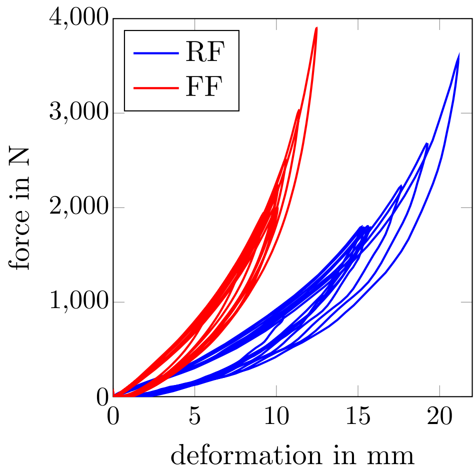

(a) SOFT

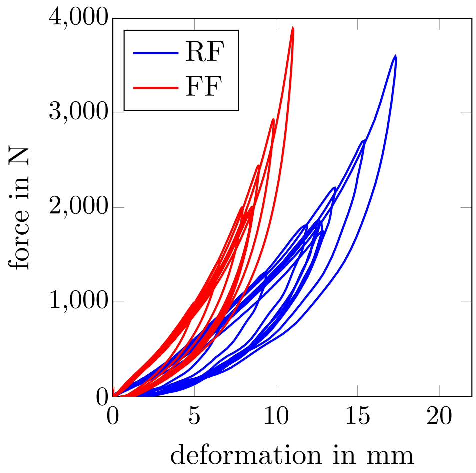

(b) CONTROL

Figure 3.: Average force-deformation curves of running shoes with two different midsole materials, BOOST^{TM} (SOFT) (a) and ethyl vinyl acetate (CONTROL) (b). Different measurements were performed for the rearfoot (RF) (blue) and forefoot (FF) (red) according to Tab. 1.

a slower measurement for the RF and a faster measurement for the FF using the respective other default setting. This ensured a more valid range of the fitted model in Sec. 2.1.2 as during the optimal control simulation unrealistically high or low values could appear. We performed 20 repetitions for each test setup and averaged the trials afterwards. All averaged force-deformation measurements (Fig. 3) were then used to identify the stiffness and damping coefficients of the contact elements as described in the following section 2.1.2.

2.1.2. Curve Fitting

At each contact point, we formulated the vertical contact force, F_y, as a nonlinear function of the deformation d, and the deformation rate $\dot{d}$. We enhanced the contact model of Gerritsen et al. (1995) by linear and nonlinear terms until the best fit to the measurement data was obtained. This resulted in the third-order relationship

$$F_y = \alpha_1 d + \alpha_2 d^2 + \alpha_3 d^3 + \beta d \dot{d}, \tag{1}$$

with the stiffness parameters α_1, α_2, and α_3 and the damping factor β. Four parameter sets were determined, for the RF and FF each for SOFT and CONTROL. The parameter sets were found by least-squares fitting of the corresponding measurements.

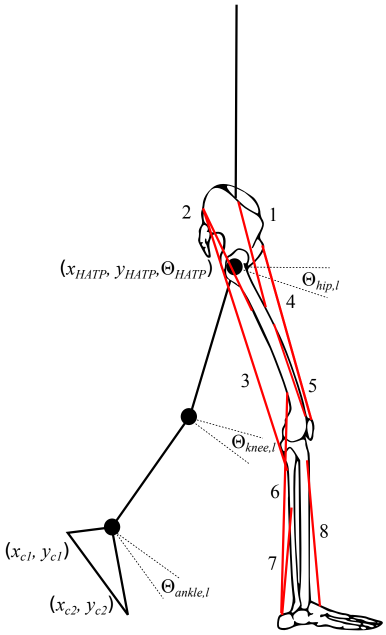

Figure 4.: Schematic representation of the musculoskeletal model with seven rigid segments: head-arms-trunk-pelvis (HATP), left and right thigh, shank and foot, and 16 Hill-type muscles: 1 - iliopsoas, 2 - glutei, 3 - hamstrings, 4 - rectus femoris, 5 - vasti, 6 - gastrocnemius, 7 - soleus, 8 - tibialis anterior. The model has nine kinematic degrees of freedom: The joint angles ($\Theta_{hip,l/r}, \Theta_{knee,l/r}, \Theta_{ankle,l/r}$) and the global position and orientation of the HATP segment ($x_{HATP}, y_{HATP}, \Theta_{HATP}$).

2.2. Simulation Study

We compared the influence of the two midsole materials on the running performance of 280 virtual runners. We created 280 musculoskeletal models and simulated running for SOFT and CONTROL midsoles by solving optimal control problems. First, we explain the musculoskeletal model and optimal control simulation (see Sec. 2.2.1 and 2.2.2). Then, we describe the virtual study design in Sec. 2.2.3.

2.2.1. Musculoskeletal Model

Each model consisted of seven rigid segments, one head-arms-trunk-pelvis segment, and three segments for each lower extremity: thigh, shank, and one segment for the foot (see Fig. 4). We scaled the segments' masses, lengths, centers of masses, and moments of inertia based on the height and weight according to Winter (2009). We applied Kane's method using Autolev 4.1 (Symbolic Dynamics Inc., Sunnyvale, California, USA) to derive multibody dynamics. In addition, the model had 16 muscles, eight for each lower extremity (see Fig. 4). Each muscle was modeled as three-element Hill-type model. The muscle dynamics are described in detail in previous publications (van den Bogert et al. 2011; van den Bogert et al. 2012).

In total, each model had 9 kinematic degrees of freedom, the hip, knee and ankle angles and the global position of the hip. The current state of each model was described by the state vector:

$$\mathbf{x} = \begin{pmatrix} \mathbf{q} & \text{9 generalized coordinates} \\ \dot{\mathbf{q}} & \text{9 generalized velocities} \\ \mathbf{L_{CE}} & \text{16 contractile elements lengths} \\ \mathbf{a} & \text{16 chemical muscle activations} \end{pmatrix}. \tag{2}$$

The model was driven by a control vector $\mathbf{u}$ comprising 16 neural excitations for all muscles. We implicitly formulated the system dynamics, i.e., the coupled multi-body dynamics and muscle dynamics, (van den Bogert et al. 2011):

$$f(\mathbf{x}, \dot{\mathbf{x}}, \mathbf{u}) = 0. \tag{3}$$

For the dynamic equilibrium in Eq. 3, the vertical contact force F_y was computed by Eq. 1 based on the current state of the model (Eq. 2). Therefore, the deformation d was derived from the state vector $\mathbf{x}$. The global coordinates of the contact points, (x_c, y_c), could be directly computed from the state vector $\mathbf{x}$ based on the global coordinates of the hip and the joint angles. The contact points were placed at the heel and ball area and scaled with the model's foot length l_{foot}: $(-0.2l_{foot}, -0.07\,\text{m})$ (RF) and $(0.6l_{foot}, -0.07\,\text{m})$ (FF) with respect to the ankle location. To ensure that the model is differentiable twice, as required by the optimal control methods, the deformation d was computed at each contact point by

$$d = \frac{1}{2}\left(\sqrt{y_c^2 + y_0^2} - y_c\right). \tag{4}$$

The smoothing parameter was set to $y_0 = 0.002\,\text{m}$ for a continuous transition of F_y at the ground contact $y_c = 0\,\text{m}$. Furthermore, we modeled the horizontal forces that resist slipping of the shoe relative to the ground as a continuous approximation to Coulomb friction (Gerritsen et al. 1995):

$$F_x = -\zeta F_y \frac{\dot{x}_c}{\sqrt{\dot{x}_c^2 + v_0^2}}, \tag{5}$$

with the sliding velocity $\dot{x}_c$ and the friction coefficient ζ (we set $\zeta = 1$ according to Gerritsen et al. (1995)). The smoothing parameter was set to $v_0 = 0.1\,\mathrm{m\,s^{-1}}$ for a continuous transition of F_x at zero velocity $\dot{x}_c = 0\,\mathrm{m\,s^{-1}}$.

2.2.2. *Optimal Control Simulation*

We simulated a half gait cycle assuming symmetric gait by solving an optimal control problem. The objective function was a weighted sum of muscular effort and deviation from normal running movement. The constraints were the lower and upper bounds on the state ($\mathbf{x}_L$, $\mathbf{x}_U$) and control vectors ($\mathbf{u}_L$, $\mathbf{u}_U$), the dynamic equilibrium (Eq. 3), and the task fulfillment of periodic forward movement. The motion and control trajectories were found by solving:

$$\begin{aligned}
&\min_{\mathbf{x}(t),\mathbf{u}(t)} \frac{1}{T}\int_0^T \Bigg(\underbrace{\frac{W}{16}\sum_{i=1}^{16} u_i(t)^3}_{\text{muscular effort}} + \underbrace{\frac{1}{5}\sum_{j=1}^{5}\frac{(s_j(t)-m_j(t))^2}{\sigma_j(t)^2}}_{\text{deviation from normal running}} \Bigg)\,\mathrm{d}t \\
&\text{s.t.} \quad \mathbf{x}_L \leq \mathbf{x} \leq \mathbf{x}_U \\
&\qquad\; \mathbf{u}_L \leq \mathbf{u} \leq \mathbf{u}_U \\
&\qquad\; f(\mathbf{x}(t), \dot{\mathbf{x}}(t), \mathbf{u}(t)) = 0 \\
&\qquad\; \mathbf{x}(0) + vT\mathbf{e}_x - \mathbf{x}^*(T) = 0,
\end{aligned} \tag{6}$$

where T is the duration of a half gait cycle, W is a weighting factor and s_j denotes the simulated variable with the associated measured variable m_j. We normalized the tracking term by the variance σ_j^2 of the measured variable. We tracked the hip angle, knee angle, ankle angle, and the vertical and horizontal GRF of a public dataset of running biomechanics (see Sec. 2.2.3). We allowed a deviation of the tracked movement by increasing the weighting $W = [1, 10, 100, 1000]$ of the effort term in the objective function (Eq. 6). The weighting W was subsequently increased to allow deviation from the tracked data. After a half period, the model had to be in the same state mirroring left and right leg $\mathbf{x}^*(T)$ plus a forward translation in direction $\mathbf{e}_x$ at speed v. We solved the optimal control problem by direct collocation with Backward Euler discretization at N time nodes (van den Bogert et al. 2011). The number of collocation nodes was set to $N = 100$ according to the sampling rate of the tracked data. We used a result of an independent running simulation (different contact model and tracking data) as initial guess. The initial guess was chosen as a good starting point to decrease computation time. We used the software library for large scale nonlinear optimization IPOPT (Wächter and Biegler 2006).

2.2.3. *Virtual Study Design*

The aim of the virtual study design was to simulate a population of runners to predict the average effect of the midsole material. Therefore, we created multiple musculoskeletal models and tracked a variability of running patterns including fore-foot, mid-foot and rear-foot striking. In this work, we used a public dataset that comprises processed biomechanics variables of 28 subjects running at $2.5\,\mathrm{m\,s^{-1}}$, $3.5\,\mathrm{m\,s^{-1}}$, and $4.5\,\mathrm{m\,s^{-1}}$ (Fukuchi et al. 2017). The distribution of the height and weight (175.2 ± 5.7 cm and 70 ± 7.1 kg) compares well to the experimental study of Worobets et al. (2014) (174.9 cm (168-186), and 71.6 kg (63.6-76.4)). This allows a direct comparison of the simulation results. First, we created 28 musculoskeletal models according to the height and weight of Fukuchi et al. (2017) using the default muscle parameters. In addition, we created 9 models for each of the 28 subjects by randomly changing the default muscle parameters to ensure that the prediction outcome is insensitive to the muscle parameters. The muscle parameters (maximal isometric force, fiber length at maximal isometric force, muscle-tendon length at neutral skeleton pose, and the moment arms at each joint) were independently drawn from a normal distribution around their default value with a standard deviation (SD) of 10%. We chose a standard deviation (SD) of 10% as a reasonable estimate of the variance between human subjects (Hasson and Caldwell 2012; Esposito and Miller 2018). The ratio between the slack length of the serial elastic element to the muscle-tendon length at neutral skeleton pose (all joint angles are zero) were fixed to a constant value. The right and left muscle parameters had always the same value. The number of randomized subjects was increased until the simulated change in energy cost converged. We tracked the running patterns of pace $v = 3.5\,\mathrm{m\,s^{-1}}$ for comparison to Worobets et al. (2014) who recorded an average speed of $3.3\,\mathrm{m\,s^{-1}}$. We used the mean and SD of the hip, knee and ankle angle, and vertical and horizontal GRF of each individual subject of Fukuchi et al. (2017). In total, 1120 optimal control problems were solved ($W = [1, 10, 100, 1000]$ for 280 subjects).

2.2.4. *Performance Estimation*

We considered three different metrics to estimate energy cost of running. We compared the muscular effort, E_{mus}, that was minimized in the objective function, i.e. the sum of the cubic muscle excitations. We compared the mechanical costs, E_{mech}, which we computed as average rate of positive work generated by the contractile elements across one gait cycle (van den Bogert et al. 2012). Moreover, we estimated the metabolic cost, E_{met}, based on a thermal energy model Umberger et al. (2003) and Umberger (2010). We computed the relative change of these performance parameters,

$$\Delta_{E_{mus}} = \left(\frac{E_{mus,SOFT}}{E_{mus,CONTROL}} - 1\right) 100\%, \tag{7}$$

$$\Delta_{E_{mech}} = \left(\frac{E_{mech,SOFT}}{E_{mech,CONTROL}} - 1\right) 100\%, \tag{8}$$

and

$$\Delta_{E_{met}} = \left(\frac{E_{met,SOFT}}{E_{met,CONTROL}} - 1\right) 100\%, \tag{9}$$

and compared it to the measured change in steady-state oxygen consumption, $\Delta_{E_{VO2}}$, of Worobets et al. (2014). We applied a one tailed paired-sample t-test for significance analysis. We examined whether running with SOFT midsoles requires less energy than running with CONTROL midsoles. Therefore, we tested the hypothesis that the mean of E_{mus}, E_{mech} and E_{met} for SOFT midsoles is significantly less than for CONTROL midsoles using a significance level of 5%.

Finally, we estimated the dissipated energy (energy loss) in footwear calculating

Table 2.: Curve fitting results: Square of the multiple correlation coefficient, R^2 and resulting model parameters for the midsole materials BOOST™ (SOFT) and ethyl vinyl acetate (CONTROL), for the contact points at the rearfoot (RF) and forefoot (FF).

	R^2	$\alpha_1\left(\frac{\mathrm{N}}{\mathrm{mm}}\right)$	$\alpha_2\left(\frac{\mathrm{N}}{\mathrm{mm}^2}\right)$	$\alpha_3\left(\frac{\mathrm{N}}{\mathrm{mm}^3}\right)$	$\beta\left(\frac{\mathrm{Ns}}{\mathrm{mm}^2}\right)$
SOFT-RF	0.990	27.48	2.80	0.14	0.03
SOFT-FF	0.993	111.50	−6.63	1.67	0.15
CONTROL-RF	0.986	42.28	4.01	0.24	0.07
CONTROL-FF	0.988	111.30	−3.24	2.02	0.29

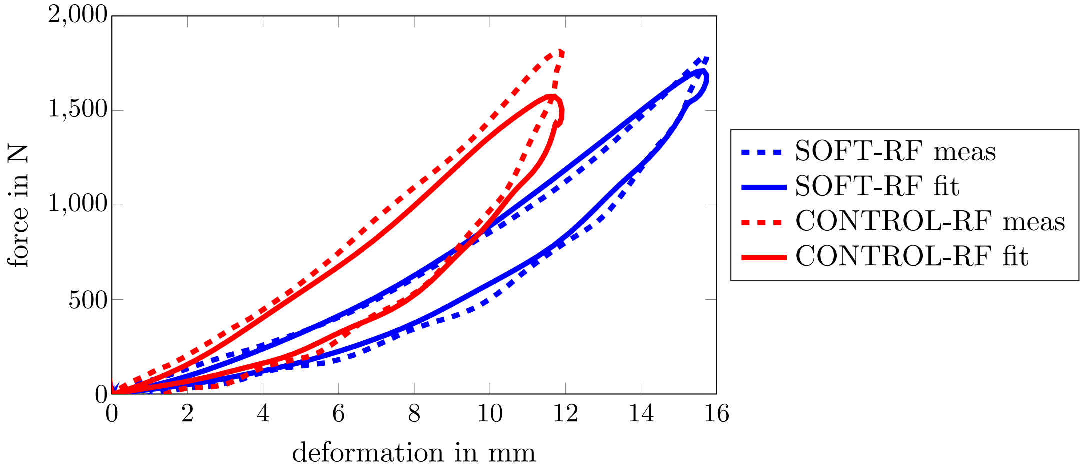

Figure 5.: Fitting of the ground-contact model (Eq. 1) to measurements for the rearfoot (RF) of the two midsole materials, BOOST™ (SOFT) and ethyl vinyl acetate (CONTROL) (RF-1 in Tab. 1).

the enclosed area by the hysteresis loop of the force-displacement graphs. This was done for the measurements in Tab. 1 adding the energy loss of the related RF and FF tests. In addition, we estimated the energy loss for the 280 simulations adding up the enclosed areas of the vertical force F_y over the displacement d of the two contacts points at the right foot. We tested for significance between the two midsole materials using a one tailed paired-sample t-test and a significance level of 5%.

3. Results

3.1. Ground-Contact Model

The goodness of fit and the fitted coefficients of Eq. 1 are listed in Tab. 2. Fig. 5 shows an example of the model identification for the setting RF-1 of SOFT and CONTROL (Tab. 1).

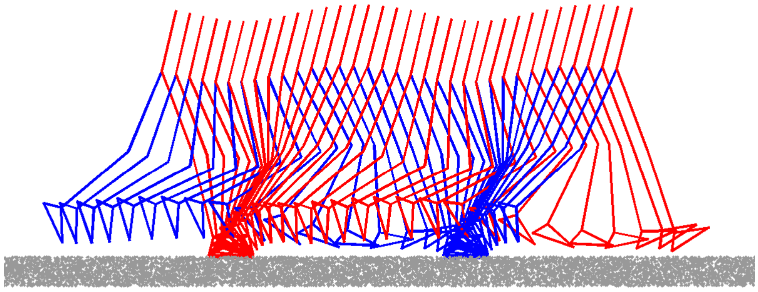

Figure 6.: Musculoskeletal model simulated at $v = 3.5\,\mathrm{m\,s^{-1}}$.

3.2. Virtual Study

We solved the optimal control problem (Eq. 6) for 280 musculoskeletal models. All simulations converged within ∼1min-1h (increasing with W) on an Intel Xeon E5-1660 v4 processor. Fig. 6 shows an exemplary resulting running movement. The average pattern across all models of the GRF, joint angles, moments, and muscle forces is depicted in Fig. 7 (for $W = 100$). The mean and one SD are plotted in blue and red for SOFT and CONTROL midsoles, respectively. One SD of the mean tracked variables is shaded in grey. The maximum knee moment is significantly higher for running with CONTROL for all considered values of W. The movement patterns for $W = 1$ follow more closely the tracked data with higher muscle excitations. For $W = 1000$, the movement patterns of musculoskeletal models were outside the measured SD of all subjects of (Fukuchi et al. 2017). Fig. 8a shows the according mean and SD of metabolic cost across all virtual subjects for varying W. The values for $W = 100$ were realistic for human running at $3.5\,\mathrm{m\,s^{-1}}$ (∼ 3 J/m/kg - 4.5 J/m/kg; Rubenson et al.). The relative change in percentage of the performance measures for $W = 100$ were: $\Delta_{E_{mus}} = -1.7 \pm 1.8\%$, $\Delta_{E_{mech}} = -0.6 \pm 1.9\%$ and $\Delta_{E_{met}} = -0.7 \pm 1.5\%$. The boxplot in Fig. 8b illustrates the relative change for $W = 100$ and shows the comparison to Worobets et al. (2014) (shaded in blue). The performed ttest indicated that the mean of the performance parameters is significantly higher for CONTROL than for SOFT ($p < 0.05$) for all considered W for E_{mech} (p = 8.5e-09, 2.9e-06, 1.2e-07, 4.3e-03) and E_{met} (p = 5.4e-06, 9.0e-12, 3.2e-12, 2.0e-07) and for $W = 100$ and $W = 1000$ for E_{mus} (p = 0.5, 0.4, 4.6e-19, 1.8e-16). To explain the energy savings, Tab. 3 summerizes the results for each individual muscle. The average muscle activation, E_{mech} and E_{met}

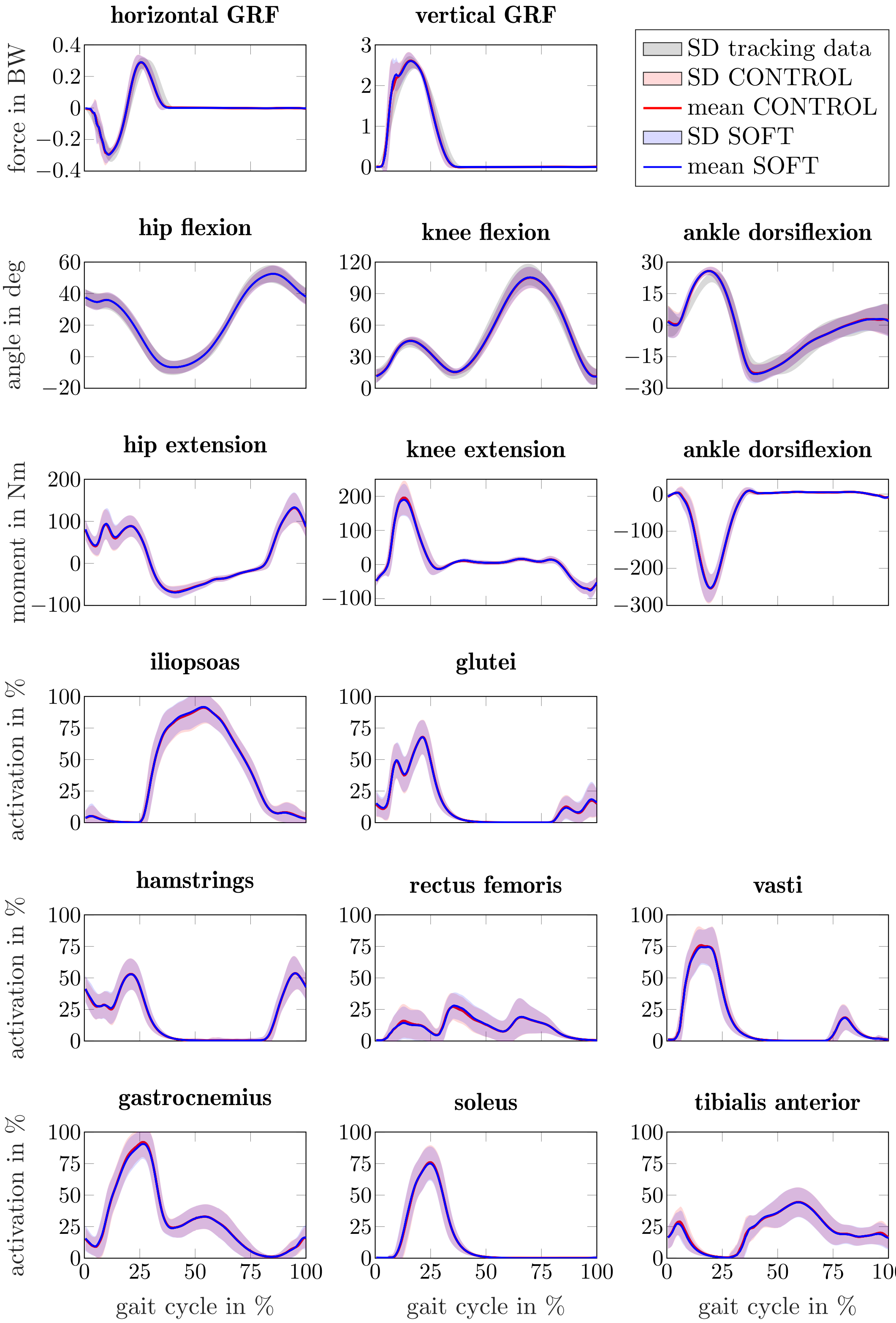

Figure 7.: Average ground reaction force (GRF), joint angles, joint moments, muscle excitations across all virtual runners. The mean and one standard deviation (SD) of simulated running with BOOST^{TM} (SOFT) and ethyl vinyl acetate (CONTROL) midsoles are plotted in blue and red, respectively. One SD of the mean tracked variables is shaded in grey.

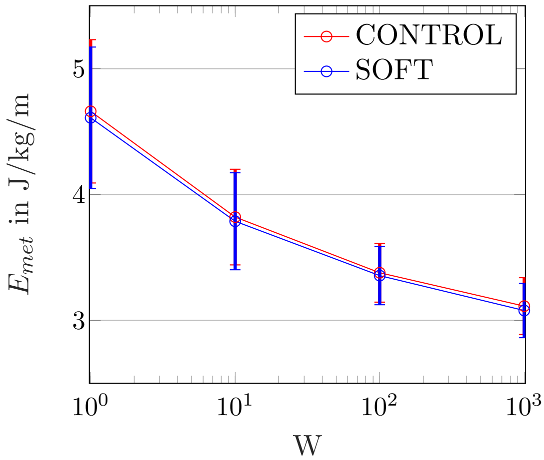

(a) Mean ± SD across all virtual subjects.

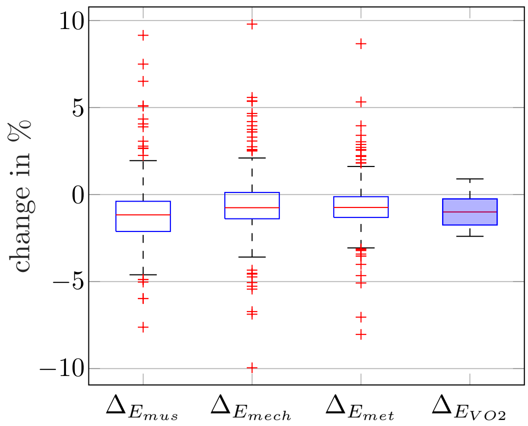

(b) Reduction in energy cost ($W = 100$).

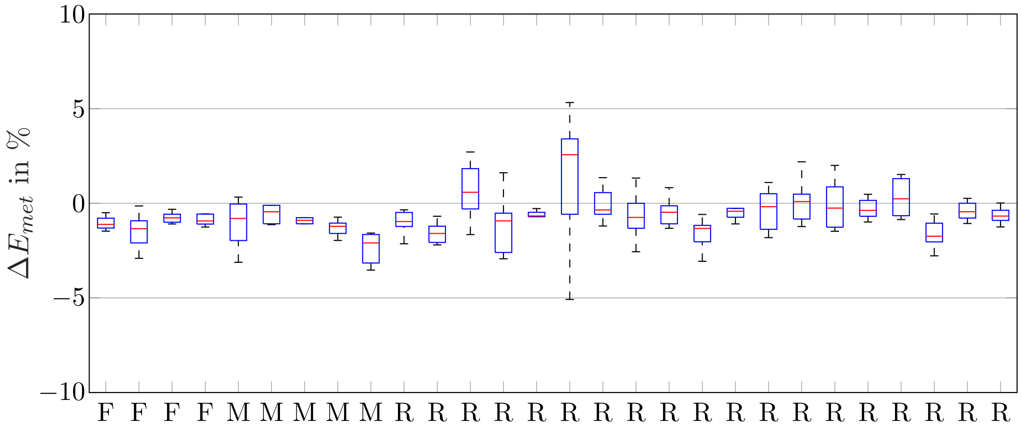

(c) Boxplot differentiating 28 tracked running patterns including fore-foot (F), mid-foot (M) and rear-foot (R) striking ($W = 100$).

Figure 8.: Comparison of simulated and measured decrease of energy cost when running with SOFT compared to CONTROL midsoles. Fig. 8a shows the mean and standard deviation (SD) of metabolic cost, E_{met}, across all virtual subjects. In Fig. 8b, the transparent box plots show the simulated change of muscular effort (E_{mus}), mechanical work (E_{mech}) and metabolic cost (E_{met}). The shaded box plot shows the measured change of oxygen consumption (E_{VO2}) for treadmill running taken from Worobets et al. (2014). Fig. 8c depicts the changes in E_{met} separately for the different tracking data of Fukuchi et al. (2017).

Table 3.: Across one gait cycle: Average muscle activation (a), average rate of positive work generated by the contractile element of each muscle (E_{mech}) and average metabolic cost (E_{met}). Significant lower values for either of the two materials are printed in bold ($p < 0.05$).

	a (%)		E_{mech} (W)		E_{met} (J/kg/m)	
	SOFT	CONTROL	SOFT	CONTROL	SOFT	CONTROL
iliopsoas	37.62±5.19	37.58±5.29	**32.64±5.32**	32.76±5.27	**0.294±0.046**	0.295±0.045
glutei	14.80±2.78	**14.75±2.72**	41.32±10.13	41.45±10.32	**0.335±0.073**	0.336±0.074
hamstrings	18.15±3.08	**18.01±3.08**	30.38±9.02	**30.02±8.91**	0.205±0.050	**0.203±0.049**
rectus femoris	11.28±3.61	11.22±3.59	3.22±1.28	3.21±1.28	0.035±0.013	0.035±0.012
vasti	**15.60±2.59**	15.83±2.60	**32.79±9.20**	33.45±9.55	**0.379±0.075**	0.385±0.076
gastrocnemius	**30.19±4.97**	30.38±4.97	**23.54±6.50**	23.70±6.31	**0.206±0.043**	0.208±0.043
soleus	13.55±2.58	13.51±2.58	**15.92±5.59**	16.34±5.72	**0.115±0.037**	0.117±0.038
tibialis anterior	**21.19±4.77**	21.55±4.70	**13.41±4.54**	13.52±4.52	**0.110±0.031**	0.111±0.031

of each individual muscle are listed for $W = 100$ and significant energy savings are marked bold. In Fig. 8c, the relative change in E_{met} is shown separately for the 28 tracking data sets of Fukuchi et al. (2017). For four tracking data sets (all rear-foot strike patterns), the relative change of E_{met} was greater than zero. In total, SOFT midsoles reduced E_{met} for 218 out of 280 virtual subjects. This is equivalent to (Worobets et al. 2014) who measured a positive effect for $\sim 80\%$ of their subjects. However, they did not screen their subjects for foot-strike style.

The measured energy loss in the midsole material was significantly different (p=5.7e-04): $7.5 \pm 3.2J$ for CONTROL and $6.2 \pm 2.4J$ for SOFT ($14.9 \pm 8.1\%$ lower). The simulated energy loss was also significantly different (p=2.7e-123): $5.2 \pm 1.3J$ for CONTROL and $4.4 \pm 1.2J$ for SOFT ($15.4 \pm 5.5\%$ lower).

4. Discussion

Previous work (Gerritsen et al. 1995; Wright et al. 1998) was limited to the impact phase of running and assumed that muscle activations remained the same when footwear was changed. Full cycle running was simulated by Hamner et al. (2010) and Hamner and Delp (2013), but they generated a subject-specifc simulation based on measured marker trajectories and ground reaction forces. The simulation was not predictive and thus not suitable for our purpose. We simulated a symmetric gait cycle and predicted muscle activations and motion trajectories simultaneously for different midsole materials.

4.1. Ground-Contact Model

We presented a novel ground-contact model to capture shoe characteristics. We chose discrete visco-elastic elements for modeling the contact mechanics. Our approach is based on previous work (Gerritsen et al. 1995; Cole et al. 1996; Wright et al. 1998). The proposed contact model yields better fitting results than the model presented by Gerritsen et al. (1995). It leads to similar fitting results as the model presented by Wright et al. (1998), but the presented model is differentiable as required for optimal control simulations. In section 2.1.1, we described the performed load-displacement measurements to imitate heel-to-toe running. We used 10 different measurement setups to cover a high variety of ground reaction force patterns (Nigg 2010). We chose a wide range for F_{max} to ensure that the model is valid in its edge regions. The hysteresis curves in Fig. 3 show that the material response is almost identical for the varied un-/loading velocities. Thus, the three measurement setups with different impact velocities seem to be sufficient for identifying the model. This work is a first evaluation of predictive simulation in sports shoe design. Future work will consider more complex contact models which incorporate the coupling between contact points, e.g., using finite element models. Moreover, we would like to identify a model capable to represent a variety of running shoes. Then, the product developer can optimize design parameters by adding them as unknowns to the state vector of the optimal control simulation.

4.2. Virtual Study

We presented a methodology how to perform a virtual study in order to replace or complement experimental studies. The optimal control simulation predicts the same trend as experimental studies: running with SOFT decreases energy cost of running by about 1%. In experimental studies, a decrease of steady-state VO_2 ($\mathrm{mol\,kg\,min^{-1}}$) of $\sim 1\%$ was measured (Worobets et al. 2014). Unfortunately, no VCO_2 measures were available for direct comparison of metabolic cost. Moreover, it needs to be examined how this difference affects race times. However, the purpose of this work was to evaluate whether the simulation framework can predict the same trend as experimental studies. Future work can run different simulations without prescribing the speed and minimizing the race time in the objective function.

We simulated a study with 280 virtual runners by changing the models' height, weight, and muscle parameters. We showed that the results are insensitive to model parameter variations. Changing the muscle parameters with a SD of 10% proved to be adequate as the resulting change in energy cost had a similar SD as measured by Worobets et al. (2014) and only few outliers were apparent. A subject-specific prediction would require a more differentiated model scaling. However, this study aimed to predict a general effect of midsole materials and we will examine subject-specific effects in the future for individualizing footwear.

The simulation is not purely predictive as we used a tracking term in our objective function. We are not aware of any simulation method that can predict realistic running patterns without tracking data. However, with proper weighting of an effort term, data tracking can produce simulations that are both realistic and predictive (van den Bogert et al. 2012). In this study, the weighting of the effort term W (in the objective function) was varied to find a trade-off between realistic movement and prediction of new motion patterns. We increased the weighting on the effort term to allow more deviation from the tracking data. Equal weighting of tracking and effort term, $W = 1$, yielded unnatural on/off switching of the muscles to match the tracking data. The models expended much more energy to cushion the first impact, because the impact peak in the tracked data was smoothed by averaging multiple gait cycles. The predicted metabolic cost was in a realistic range for $W = 100$. The weighting $W = 1000$ led to running movements that were outside the range of measurements and delivered unrealistically low metabolic cost. In future work, we will investigate new cost functions like the direct minimization of metabolic energy and inverse optimal control (Mombaur et al. 2010) to avoid tracking. In this work, we used a wide range of tracking data to make sure that the performance measures are insensitive to the tracked motion.

The simulation gives insight to several parameters which are not directly measurable or not considered during experiments like muscle controls, joint kinematics, and kinetics. The simulation suggests that the peak knee extension moment is significantly reduced for the SOFT midsole while increasing hamstrings contraction. The models ran with greater forward trunk lean. They landed further back on their foot, but shifted their weight faster to the forefoot. This required more force in the hamstrings but less force in the vasti muscles. This was not yet evaluated in experiments. Moreover, we found that iliopsoas, glutei, vasti, gastrocnemius, soleus, and tibialis anterior muscles produced less mechanical energy cost. The virtual subjects could benefit from SOFT midsoles during the whole gait cycle. Most energy was saved during propulsion ($15 - 35\%$ of the gait cycle) as vasti, gastrocnemius and soleus muscles were less activated in this phase. This is probably due to the fact that about 15% less energy was dissipated in the midsole material for the SOFT midsole and thus more mechanical energy was returned compared with the amount of energy applied. Furthermore, the model pushed off the ground easier with SOFT midsoles as the peak eccentric power in the tibialis anterior muscles was $\sim 9W$ lower. In the swing phase, energy cost was slightly reduced in iliopsoas muscles.

In the future, the simulation can be used as indication which design parameters have most impact on energy cost and injury risk. Experimental studies can be conducted on these findings to save time and costs. We will investigate athlete-specific simulations to optimize design parameters individually. In addition, the method can be transferred to other domains, e.g. for designing prostheses or other medical devices. In conclusion, our approach has the potential to replace or complement experimental studies and to increase the product quality, as effects of novel design concepts could be predicted before they have been prototyped and tested.

Acknowledgement

The authors thank Anne Koelewijn, who implemented the model of muscle energy expenditure. This study was supported by a contract from adidas AG with Friedrich-Alexander-Universität Erlangen-Nürnberg, Germany. Eva Dorschky gratefully acknowledges the support of the Bavarian Ministry for Economic Affairs, Infrastructure, Transport and Technology within the Embedded Systems Initiative (ESI). Björn Eskofier gratefully acknowledges the support of the German Research Foundation (DFG) within the framework of the Heisenberg professorship programme (grant number ES 434/8-1).

Conflict of Interest Statement

Eva Dorschky, Daniel Krüger, Nicolai Kurfess, Sandro Wartzack and Björn M. Eskofier have no conflicts of interest relevant to the content of this article. Heiko Schlarb is an employee of adidas AG. Antonie J. van den Bogert is a paid consultant to adidas AG.

References

J. T.-M. Cheung and M. Zhang. Finite element modeling of the human foot and footwear. In *ABAQUS Users' Conference*, pages 145–159, 2006.

G. K. Cole, B. M. Nigg, and K. G. M. Gerritsen. Lower extremity joint loading during impact in running. *Clinical Biomechanics*, 11(4):181–193, 1996.

T. W. Dorn, J. M. Wang, J. L. Hicks, and S. L. Delp. Predictive simulation generates human adaptations during loaded and inclined walking. *PloS one*, 10(4), 2015.

E. R. Esposito and R. H. Miller. Maintenance of muscle strength retains a normal metabolic cost in simulated walking after transtibial limb loss. *PloS one*, 13(1), 2018.

R. K. Fukuchi, C. A. Fukuchi, and M. Duarte. A public dataset of running biomechanics and the effects of running speed on lower extremity kinematics and kinetics. *PeerJ*, 5, 2017.

K. G. M. Gerritsen, A. J. van den Bogert, and B. M. Nigg. Direct dynamics simulation of the impact phase in heel-toe running. *Journal of Biomechanics*, 28(6):661–668, 1995.

S. Hamner, a. Seth, and S. Delp. Muscle contributions to propulsion and support during running. *Journal of biomechanics*, 43(14):2709–2716, 2010.

S. R. Hamner and S. L. Delp. Muscle contributions to fore-aft and vertical body mass center accelerations over a range of running speeds. *Journal of biomechanics*, 46(4):780–787, 2013.

I. Hannah, A. Harland, D. Price, H. Schlarb, and T. Lucas. Evaluation of a kinematically-driven finite element footstrike model. *Journal of Applied Biomechanics*, 32(3):301–305, 2016.

C. J. Hasson and G. E. Caldwell. Effects of age on mechanical properties of dorsiflexor and plantarflexor muscles. *Annals of biomedical engineering*, 40(5):1088–1101, 2012.

W. Hoogkamer, S. Kipp, B. A. Spiering, and R. Kram. Altered running economy directly translates to altered distance-running performance. *Med Sci Sports Exerc*, 48(11):2175–80, 2016.

S. Kim, J. Cho, J. Choi, S. Ryu, and W. Jeong. Coupled foot-shoe-ground interaction model to assess landing impact transfer characteristics to ground condition. *Interaction and Multiscale*

Mechanics, 5(1):75–90, 2012.

Y.-C. Lin, J. P. Walter, and M. G. Pandy. Predictive simulations of neuromuscular coordination and joint-contact loading in human gait. *Annals of biomedical engineering*, pages 1–12, 2018.

R. H. Miller and J. Hamill. Computer simulation of the effects of shoe cushioning on internal and external loading during running impacts. *Computer Methods in Biomechanics and Biomedical Engineering*, 12(4):481–490, 2009.

R. H. Miller and J. Hamill. Optimal footfall patterns for cost minimization in running. *Journal of Biomechanics*, 48(11):2858–2864, 2015.

K. Mombaur, A. Truong, and J.-P. Laumond. From human to humanoid locomotion–an inverse optimal control approach. *Autonomous robots*, 28(3):369–383, 2010.

B. M. Nigg. *Biomechanics of sport shoes.* University of Calgary, 2010.

B. M. Nigg, J. Vienneau, A. C. Smith, M. B. Trudeau, M. Mohr, and S. R. Nigg. The preferred movement path paradigm: influence of running shoes on joint movement. *Medicine & Science in Sports & Exercise*, 49(8):1641–1648, 2017.

J. Rubenson, D. B. Heliams, S. K. Maloney, P. C. Withers, D. G. Lloyd, and P. A. Fournier. Reappraisal of the comparative cost of human locomotion using gait-specific allometric analyses. *The Journal of Experimental Biology*, 210:3513–3524.

B. R. Umberger. Stance and swing phase costs in human walking. *Journal of the Royal Society Interface*, 7(50):1329–1340, 2010.

B. R. Umberger, K. G. Gerritsen, and P. E. Martin. A Model of Human Muscle Energy Expenditure. *Computer Methods in Biomechanics and Biomedical Engineering*, 6(2):99–111, 2003.

A. J. van den Bogert, D. Blana, and D. Heinrich. Implicit methods for efficient musculoskeletal simulation and optimal control. *Procedia IUTAM*, 2:297–316, 2011.

A. J. van den Bogert, M. Hupperets, H. Schlarb, and B. Krabbe. Predictive musculoskeletal simulation using optimal control: effects of added limb mass on energy cost and kinematics of walking and running. *Proceedings of the Institution of Mechanical Engineers, Part P: Journal of Sports Engineering and Technology*, 226(2):123–133, 2012.

A. Wächter and L. T. Biegler. On the implementation of an interior-point filter line-search algorithm for large-scale nonlinear programming. *Mathematical Programming*, 106(1):25–57, 2006.

J. Wakeling, S. Pascual, and B. Nigg. Altering muscle activity in the lower extremities by running with different shoes. *Medicine and Science in Sports and Exercise*, 34(9):1529, 2002.

J. M. Wang, S. R. Hamner, S. L. Delp, and V. Koltun. Optimizing locomotion controllers using biologically-based actuators and objectives. *ACM Transactions on Graphics*, 31(4): 1–11, 2012.

D. A. Winter. *Biomechanics and motor control of human movement*. John Wiley & Sons, 2009.

J. Worobets, J. W. Wannop, E. Tomaras, and D. Stefanyshyn. Softer and more resilient running shoe cushioning properties enhance running economy. *Footwear Science*, 6(3):147–153, 2014.

I. Wright, R. Neptune, A. J. Van den Bogert, and B. Nigg. Passive regulation of impact forces in heel-toe running. *Clinical Biomechanics*, 13(7):521–531, 1998.